

AD-A270 932 N PAGE

Form Approved
OMB No. 0704-0188

2

Public use
gatherer
collector
Davis Hg



hour per response, including the time for reviewing instructions, searching existing data sources, collection of information, send comments regarding this burden estimate or any other aspect of this report to Washington Headquarters Services, Directorate for Information Operations and Reports, 1215 Jefferson Avenue, Washington, DC 20503.

1. AGENCY USE ONLY (Leave blank)

September 25, 1993

3. REPORT TYPE AND DATES COVERED

Final Report: 8/1/92 to 7/31/93

4. TITLE AND SUBTITLE

The Fluid Mechanics of Vortex Cutting By a Blade

5. FUNDING NUMBERS (G)

DAAL03-92-G-0277

6. AUTHOR(S)

Jeffrey S. Marshall

7. PERFORMING ORGANIZATION NAME(S) AND ADDRESS(ES)

Florida Atlantic University
Boca Raton, Florida 33431

DTIC
ELECTE
OCT 20 1993
S B D

8. PERFORMING ORGANIZATION
REPORT NUMBER

9. SPONSORING/MONITORING AGENCY NAME(S) AND ADDRESS(ES)

U. S. Army Research Office
P. O. Box 12211
Research Triangle Park, NC 27709-2211

10. SPONSORING/MONITORING
AGENCY REPORT NUMBER

30168.5-EG-YIP

11. SUPPLEMENTARY NOTES

The view, opinions and/or findings contained in this report are those of the author(s) and should not be construed as an official Department of the Army position, policy, or decision, unless so designated by other documentation.

12a. DISTRIBUTION/AVAILABILITY STATEMENT

Approved for public release; distribution unlimited.

12b. DISTRIBUTION CODE

13. ABSTRACT (Maximum 200 words)

A study of the nonlinear response of a vortex to the approach of, and cutting by, a blade traveling in the plane normal to the vortex axis has been performed. Two different types of vortex forces on the blade are distinguished. For large values of the ratio of blade thickness T to vortex ambient core radius σ_0 , the force on the blade is primarily due to decreased pressure near the blade leading edge due to bending of the vortex about the blade. For values of T/σ_0 of $O(1)$ or less, the vortex does not bend substantially during interaction with the blade and instead the blade passes through, or 'cuts', the vortex. In this case, the force on the blade is primarily due to formation of a "vortex shock" which propagates on the vortex away from the blade, and the subsequent difference in vortex core radius on opposite sides of the blade due to the vortex shock. This study was conducted based on analytical, computational and experimental studies, the results of which compared well in the regimes in which each are valid.

14. SUBJECT TERMS

Vortex Cutting, Blade-Vortex Interaction, Vortex Reconnection

15. NUMBER OF PAGES
30

16. PRICE CODE

17. SECURITY CLASSIFICATION
OF REPORT

UNCLASSIFIED

18. SECURITY CLASSIFICATION

UNCLASSIFIED

19. SECURITY CLASSIFICATION
OF ABSTRACT

UNCLASSIFIED

20. LIMITATION OF ABSTRACT

UL

93-24820

**Best
Available
Copy**

THE VIEWS, OPINIONS, AND/OR FINDINGS CONTAINED IN THIS REPORT ARE THOSE OF THE AUTHOR(S) AND SHOULD NOT BE CONSTRUED AS AN OFFICIAL DEPARTMENT OF THE ARMY POSITION, POLICY, OR DECISION, UNLESS SO DESIGNATED BY OTHER DOCUMENTATION.

TABLE OF CONTENTS

	<u>Page</u>
LIST OF FIGURES	ii
1. Statement of the Problem.....	1
2. Summary of the Most Important Results.....	3
a) Theoretical results	3
b) Computational results	7
c) Experimental results.....	12
d) Conclusions	21
LIST OF PUBLICATIONS AND TECHNICAL REPORTS	23
LIST OF PARTICIPATING SCIENTIFIC PERSONNEL	24
REPORT OF INVENTIONS	24
BIBLIOGRAPHY	25

DTIC QUALITY INSPECTED 2

Accession For		
NTIS GRA&I	<input checked="" type="checkbox"/>	
DTIC TAB	<input type="checkbox"/>	
Unannounced	<input type="checkbox"/>	
Justification		
By		
Distribution/		
Availability Codes		
Avail and/or		
Dist	Special	
A-1		

LIST OF FIGURES

		<u>Page</u>
1.	Schematic of vortex cutting by a flat-plate blade at angle of attack α	2
2.	Prediction for the ratio of vortex core radius σ_B near the blade to the ambient core radius σ_0 both for expansion cases (solid curve) and for compression cases (dashed curve).....	6
3.	Side view (looking along the blade span) of a vortex with axial flow rate $2\pi w_0 \sigma_0 / \Gamma = -1/2$ after cutting by a blade with angle of attack $\alpha = 0^\circ$ forward speed $2\pi U \sigma_0 / \Gamma = 1$ and thickness $T/\sigma_0 = 1$. A shock forms on the vortex above the blade and an expansion wave forms on the vortex below the blade	8
4.	Magnitude of the vortex force F_B on the blade as a function of time for the same parameter values as in Fig. 3. The solid curve is the result of the numerical computation and the dashed curve is the analytical prediction. The sudden jump in F_B coincides with the cutting of the vortex by the blade	9
5.	Side view showing bending (prior to cutting) of a vortex with zero axial flow caused by interaction with a fairly thick blade, with $T/\sigma_0 = 5$ and $2\pi U \sigma_0 / \Gamma = 1$, at zero angle of attack.....	10
6.	Side view showing the same case as in Fig. 5, but for a blade with angle of attack $\alpha = -15^\circ$	11
7.	Side view (looking down the cylinder axis) showing reconnection of the vortex with its image across the cylinder surface for a case with $T/\sigma_0 = 10$, $w_0 = 0$ and slow cylinder forward speed ($2\pi U \sigma_0 / \Gamma = 0.05$)	13
8.	Side view showing the bending of a vortex with no axial flow caused by interaction with a circular cylinder for a case with $T/\sigma_0 = 10$ and a larger cylinder forward speed ($2\pi U \sigma_0 / \Gamma = 1/2$)	14
9.	Variation of vortex core radius with distance along the vortex axis at a series of times for the same run as shown in Fig. 8.....	15
10.	Variation of vortex core radius with distance along the vortex axis at a series of times for a case with $T/\sigma_0 = 10$ and a large cylinder forward speed ($2\pi U \sigma_0 / \Gamma = 2$). Comparison of Fig. 9 and 10 shows the effect of cylinder forward speed on decrease in vortex core radius.....	16

11. Schematic of the experimental configuration: A, tow carriage driven by variable speed motor; B, water inlet into azimuthally oriented jets with optional shower head inlet; C, outer rectangular tank; D, inner cylindrical tank; E, vortex core; F, gap left to allow passage of blade (or circular cylinder) with flexible plastic strips; G, orifice at tank bottom; H, thin blade (or circular cylinder) mounted at adjustable angle of attack; I, hypodermic needle to inject dye globules for circulation measurement; J, support arms for carriage 18

12. Pictures showing the structure of vortex shocks of two different forms, both generated by cutting the vortex by a thin blade with zero angle of attack. A spiral shock is shown in (a) for the case $2\pi w_0 \sigma_0 / \Gamma = -0.26$ and $2\pi U \sigma_0 / \Gamma = 0.19$. A shock with bubble-type breakdown, which spirals in a double-helix form downstream, is shown in (b) for the case $2\pi w_0 \sigma_0 / \Gamma = -0.16$ and $2\pi U \sigma_0 / \Gamma = 0.036$. The dimensionless shock speed $2\pi \sigma_0 W / \Gamma$ is found to be 0.40 in (a) and 0.61 in (b)..... 19

13. Comparison of experimental data for shock speed, plotted in terms of the dimensionless parameter $2\pi \sigma_0 (W + \alpha U) / \Gamma$, with the analytical solution (solid curve) assuming no suction of blade boundary layer fluid into the vortex. The data points for a blade with angle of attack $\alpha = 0$ are marked by a circle 'o', those for a blade with finite α are marked by a star '*', and those taken using the shower head to inlet part of the flow (for which case the vortex has high turbulence intensity) are marked by a plus sign '+' 20

The Fluid Mechanics of Vortex Cutting by a Blade

1. Statement of the Problem

A study of the cutting of a vortex by a blade, where the blade moves in a direction normal to the vortex axis, has been performed. A schematic of the problem geometry is shown in Figure 1. The main military application of this problem is to unsteady loading and sound generation caused by cutting of trailing vortices shed by the blades of a helicopter main rotor by the blades of the tail rotor. Interaction of main rotor trailing vortices with the tail rotor blades has been identified as a major source of helicopter noise in certain flight conditions (and for certain helicopter designs) by Leverton et al. (1977). The problem is also relevant to applications such as turbulent gust loading on airplane wings, ingestion of atmospheric turbulence or wake vortices by a helicopter main rotor or submarine propeller, and cavitation damage on turbine blades due to cutting of hydraulic intake vortices.

Previous work on this problem has been either experimental (Ahmadi, 1986, Cary, 1987, Weigand, 1993), or highly idealized theoretical work (Howe, 1988, 1989, Amiet, 1986) dealing mainly with acoustical aspects of the problem. The experimental work has observed sudden pressure variation on the blade surface during cutting of the vortex, as well as strong variation in core area of the vortex following the cutting. The experimental observations of the vortex response to cutting (which are given in the literature for only a small number of cases) have not been related to a theoretical description of the problem, nor has the cutting process itself been studied in detail.

The main goal of the present project is to understand the response of the vortex to cutting by the blade, and to use this understanding to develop a simple expression for the variation of force on the blade during cutting which accurately includes the vortex response. This goal has been pursued in the current work through theoretical, computational and experimental means, with extensive comparison of results obtained using different methods.

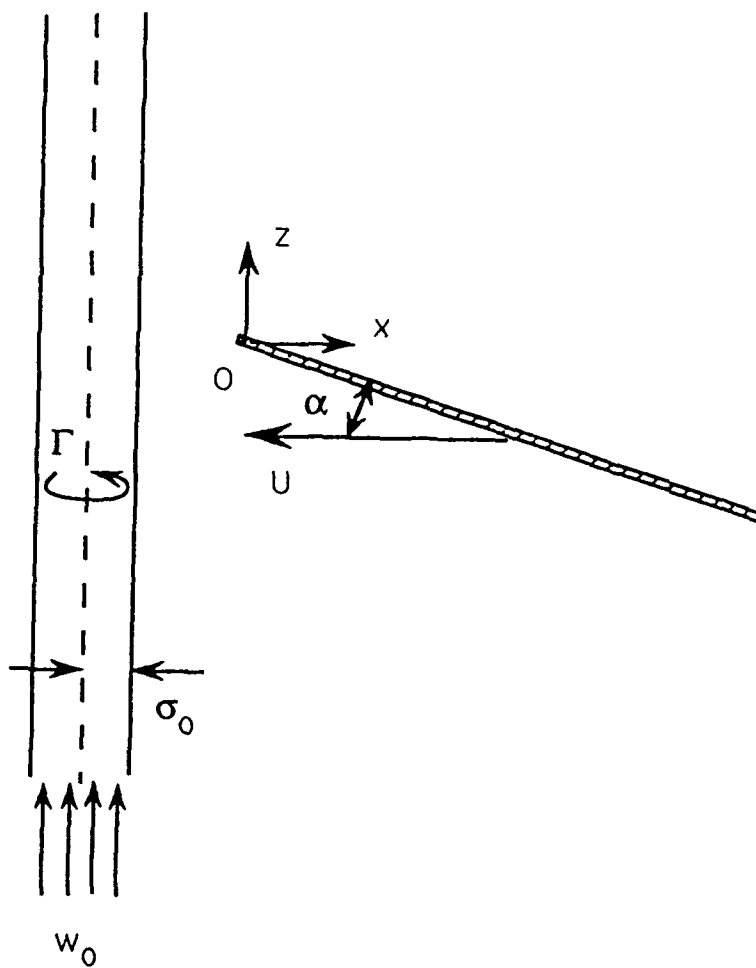


Fig. 1. Schematic of vortex cutting by a flat-plate blade at angle of attack α .

2. Summary of the Most Important Results

The results of this work have been reported in detail in four technical papers listed in Section 3. In this section, a brief summary of the main results described in these papers is given.

a) Theoretical results

A relatively recent vortex filament model (Lundgren and Ashurst, 1989, Marshall, 1991) which includes variation of vortex core area along the vortex axis, is used to solve for the vortex response to interacting with the blade, both before and after cutting. The vortex cutting process itself is assumed in the current work to occur instantaneously. In order to simplify the analytical and numerical solution of the governing equations of the vortex filament, a new long-wave approximation to these equations have been derived using a multiple time-scale perturbation method. In these long-wave equations the components (u, v, w) of velocity of the vortex centerline C in the principal normal, binormal and tangential directions, respectively, can be written in terms of the self-induced velocity components (u_I, v_I, w_I) and the induced velocity components (u_E, v_E, w_E) from the blade surface as

$$u = u_I + u_E, \quad (1)$$

$$v = v_I + v_E + \frac{\kappa\Gamma}{16\pi} - \frac{\pi\sigma^2\kappa w_A^2}{\Gamma}, \quad (2)$$

$$w = w_I + w_E + w_A, \quad (3)$$

where κ is curvature of the vortex centerline, Γ is vortex circulation, and σ is the core radius. Here σ is allowed to vary with time t and distance s along C , and is determined by the continuity requirement from

$$2\left(\frac{\partial\sigma}{\partial t} + w \frac{\partial\sigma}{\partial s}\right) + \sigma \frac{\partial w}{\partial s} - \sigma\kappa u = 0. \quad (4)$$

The self-induced velocity of the vortex is determined from the usual Biot-Savart equation (Moore, 1972), but with cut-off constant equal to that usually used for a hollow vortex since the internal forces in the core are accounted for by the other terms in (2). The velocity induced by the blade is determined by the usual vorticity panel method (Lewis, 1991). The additional axial velocity component w_A arises due to variation in pressure on the core lateral surface, caused by

variation in core radius s or by some other imposed pressure gradient. Omitting the latter effect in the current problem, w_A is given in the long-wave theory by the nonlinear hyperbolic equation

$$\sigma^2 \left(\frac{\partial w_A}{\partial t} + w \frac{\partial w_A}{\partial s} \right) = - \frac{\Gamma^2}{4\pi\sigma} \frac{\partial \sigma}{\partial s}. \quad (5)$$

We note that solution of the system (1)-(5) for the vortex motion is only slightly more difficult than solutions with the usual "cut-off" method (Moore and Saffman, 1972), involving solution of one additional differential equation (5). Unlike the usual cut-off method, however, this method has the great advantage that it includes variation in core radius along the vortex core, which arises naturally in problems of this type due to different axial stretching rates in different parts of the vortex. Computational examples using this vortex method are given in Marshall and Grant (1993) and Marshall and Yalamanchili (1993), and details of its derivation can be found in Marshall (1993b).

An analytical solution for the system (1)-(5) for the vortex response following cutting by a thin flat plate has been obtained for the special case in which the vortex axis C is a straight line. In this case, eqs. (4) and (5) reduce to

$$2 \left(\frac{\partial \sigma}{\partial t} + w \frac{\partial \sigma}{\partial s} \right) + \sigma \frac{\partial w}{\partial s} = 0, \quad (6a)$$

$$\frac{\partial w}{\partial t} + w \frac{\partial w}{\partial s} = - \frac{\Gamma^2}{4\pi\sigma^3} \frac{\partial \sigma}{\partial s}. \quad (6b)$$

The system (6) can be transformed into the one-dimensional gas dynamics equations (Lundgren and Ashurst, 1989), for which a solution can be obtained using the method of characteristics. The Riemann invariants for the system (6) are

$$\begin{aligned} J^+ &= w - 2c = \text{const on } \frac{ds}{dt} = w + c \text{ (C+ characteristics)} \\ J^- &= w + 2c = \text{const on } \frac{ds}{dt} = w - c \text{ (C- characteristics)} \end{aligned} \quad (7)$$

where the "vortex sound" speed c is given by

$$c = \left(\frac{\Gamma^2}{8\pi^2\sigma^2} \right)^{1/2}. \quad (8)$$

The problem of cutting of a straight vortex filament with ambient axial velocity w_0 and core radius σ_0 by a flat plate at angle of attack α is thus analogous to the classic problem of impulsive motion of a piston in a shock tube. The vortex response consists of propagation of a shock and an expansion wave away from the blade on opposite sides of the vortex. The axial velocity w_B within the vortex at the point of intersection of the vortex the blade (neglecting suction of blade boundary layer fluid into the vortex) is simply $w_B = -\alpha U$, where U is the speed of the blade, while sufficiently far from the blade the vortex axial velocity approaches the ambient value w_0 .

Using the solution for the vortex expansion wave, the ratio of core radius σ_B near the blade to the ambient value σ_0 is obtained for the expansion side of the vortex as

$$\frac{\sigma_B}{\sigma_0} = \frac{1}{[1 + 1/2 \left| \frac{w_0 - w_B}{c_0} \right|]} \quad (9)$$

where c_0 is the value of c with $\sigma = \sigma_0$. Using jump conditions in mass and momentum across the vortex shock, a nonlinear equation for the core radius σ_B on the compression side of the vortex is obtained as

$$\left(\frac{\sigma_B}{\sigma_0}\right)^2 (w_B - w_0)^2 = \frac{\Gamma^2}{4\pi^2 \sigma_0^2} \left(\frac{\sigma_B^2}{\sigma_0^2} - 1 \right) \ln(\sigma_B/\sigma_0). \quad (10)$$

A plot of σ_B/σ_0 for the expansion and compression sides of the vortex as obtained from (9) and (10) is given in Fig. 2. The propagation speed W of the vortex shock is obtained as a function of σ_B/σ_0 as

$$W = w_B \pm \frac{\sigma_0}{2\pi\sigma_B} \left(\frac{\Gamma^2 \ln(\sigma_B/\sigma_0)}{\sigma_B^2 - \sigma_0^2} \right)^{1/2}. \quad (11)$$

Assuming instantaneous cutting of the vortex, it is found that the jump in core radius over the blade surface produces a force normal to the blade surface and pointing toward the side of the blade on which the core radius is largest. The magnitude of this force is given by

$$F = \frac{\rho^* \Gamma^2}{4\pi} \ln(\sigma^+/\sigma^-) \quad (12)$$

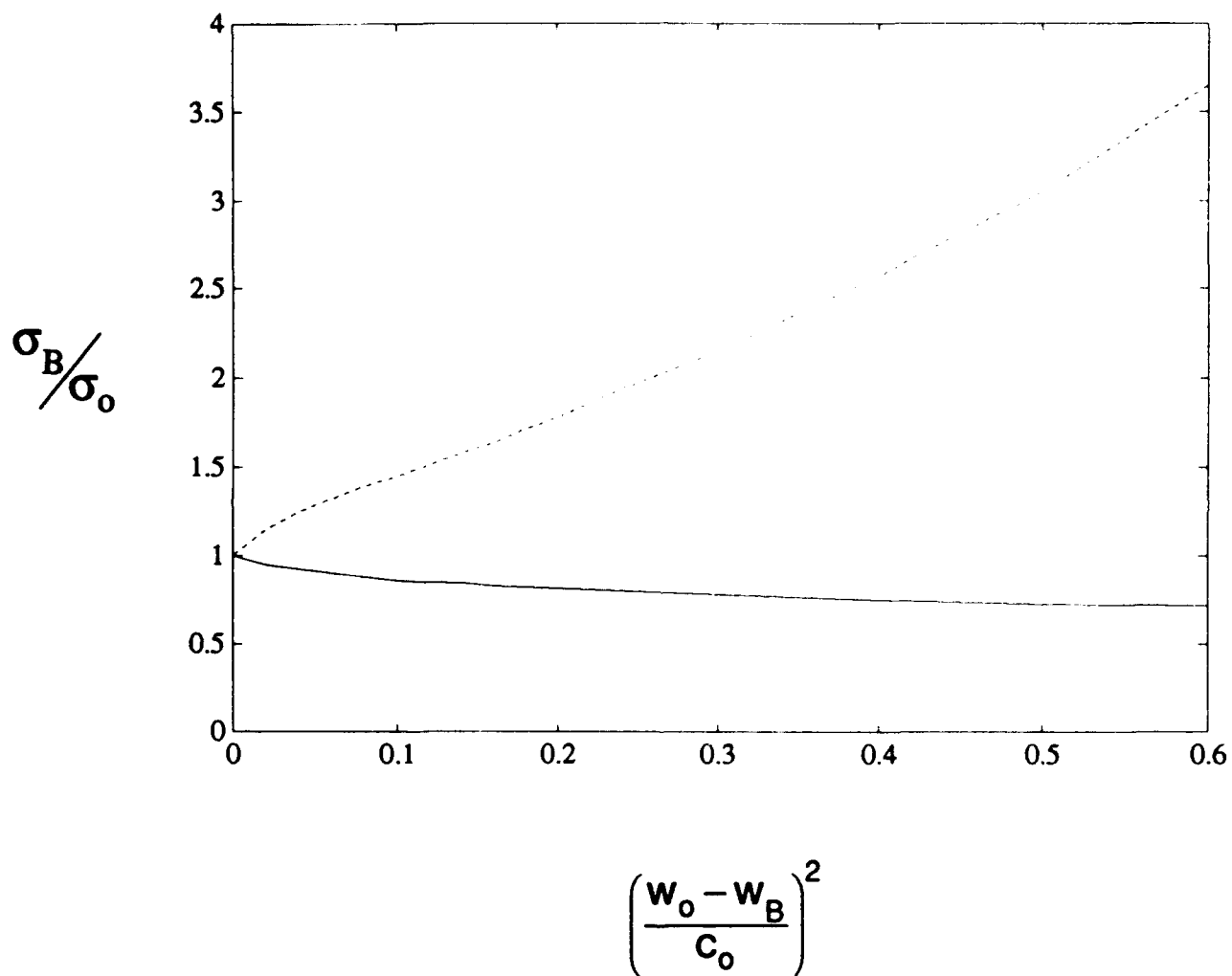


Fig. 2. Prediction for the ratio of vortex core radius σ_B near the blade to the ambient core radius σ_0 both for expansion cases (solid curve) and for compression cases (dashed curve).

where ρ^* is the fluid density and σ^+ and σ^- are the vortex core radii on the upper and lower sides of the blade, respectively. [Here the upward and downward directions are set by the assumption of positive angle of attack α .]

b) Computational results

The analytical solution given in the previous section neglects bending of the vortex that might result from interaction with the blade. In the current section, we use numerical computations of blade-vortex interaction (which include the possibility of cutting of the vortex) to investigate the nature of the vortex bending response to the blade. These computations are based on the long-wave form of the vortex filament equations given in the previous section, together with a vorticity panel representation of the blade boundary layer. Details of the computational method are given in Marshall and Yalamanchili (1993).

There are three dimensionless parameters which control the vortex response to interaction with the blade: the ratio T/σ_0 of blade thickness T to ambient core radius σ_0 , the ratio $2\pi U\sigma_0/\Gamma$ of blade-vortex relative forward speed U to vortex "swirl" velocity $\Gamma/2\pi\sigma_0$ and the angle of attack α of the blade. For cases where the thickness ratio T/σ_0 is of order unity or smaller, the computations indicate that the vortex does not bend significantly due to interaction with the blade, either before or after cutting. This result seems to hold for arbitrary values of $2\pi U\sigma_0/\Gamma$ and α (at least for $\alpha < 20^\circ$). The resulting vortex response thus closely follows the analytic solution described in the previous section. An example of vortex response to cutting is shown in Fig. 3 for a vortex with downward ambient axial flow. A vortex shock is observed on the upper (compression) side of the vortex and an expansion wave is observed on the lower (expansion) side. The lines are side views of circles drawn at initially even increments about the core. A plot of the variation of the dimensionless force on the blade versus dimensionless time is given in Fig. 4 for this case, and is observed to follow closely the analytical result (dashed line). The sudden jump in vortex force corresponds with the instant of cutting.

For values of T/σ_0 greater than about 3, significant bending of the vortex was observed prior to cutting. Examples of the vortex bending response with $T/\sigma_0 = 5$ are shown in Fig. 5 (with $\alpha = 0$) and Fig. 6 (with $\alpha = -15^\circ$), both for $2\pi U\sigma_0/\Gamma = 1$. Particularly interesting is the case with finite blade angle of attack in Fig. 6, where the vortex is observed to develop a "kink" on the low pressure side of the blade. In Fig. 6, the core radius is about 20% below ambient on one side of the kink and about 20% above ambient on the other side. As the calculation progressed, the kink became increasingly accentuated and dominated the vortex response. Such

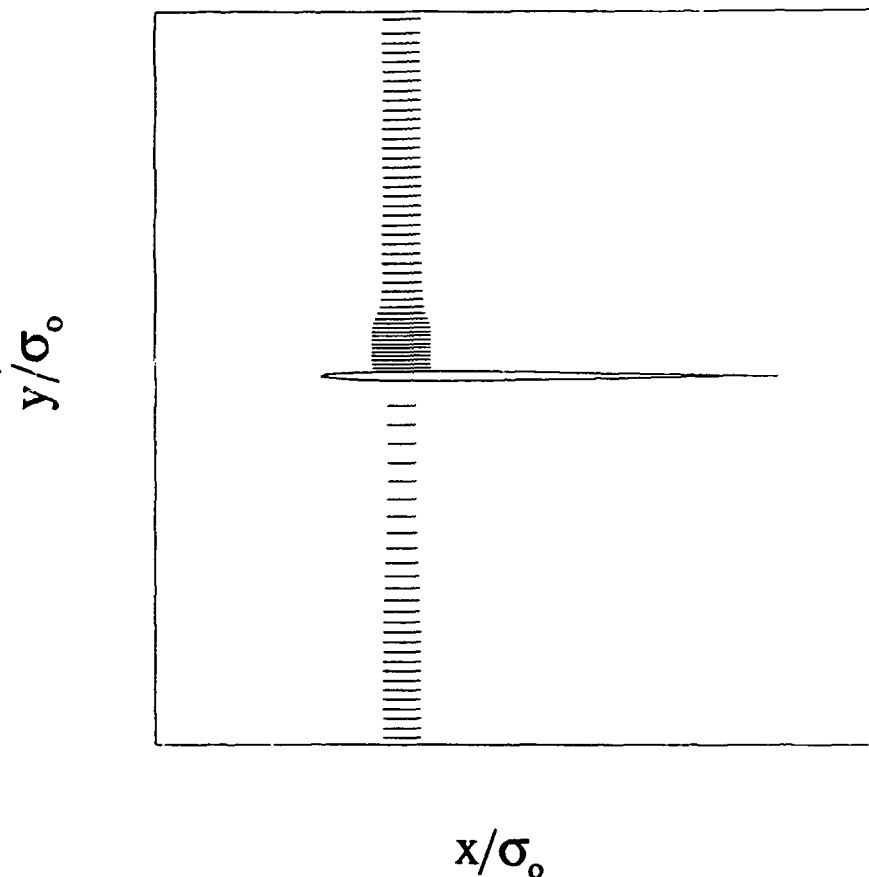


Fig. 3. Side view (looking along the blade span) of a vortex with axial flow rate $2\pi w_0 \sigma_0 / \Gamma = -1/2$ after cutting by a blade with angle of attack $\alpha = 0^\circ$ forward speed $2\pi U \sigma_0 / \Gamma = 1$ and thickness $T / \sigma_0 = 1$. A shock forms on the vortex above the blade and an expansion wave forms on the vortex below the blade.

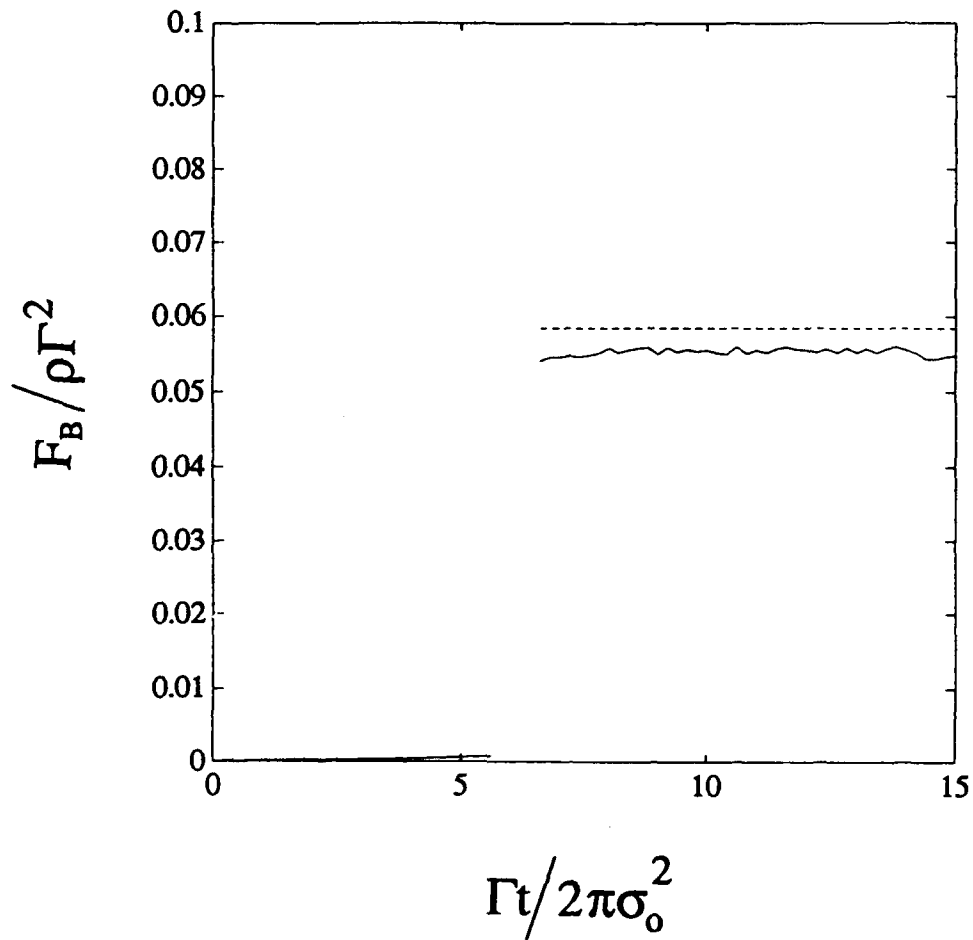


Fig. 4. Magnitude of the vortex force F_B on the blade as a function of time for the same parameter values as in Fig. 3. The solid curve is the result of the numerical computation and the dashed curve is the analytical prediction. The sudden jump in F_B coincides with the cutting of the vortex by the blade.

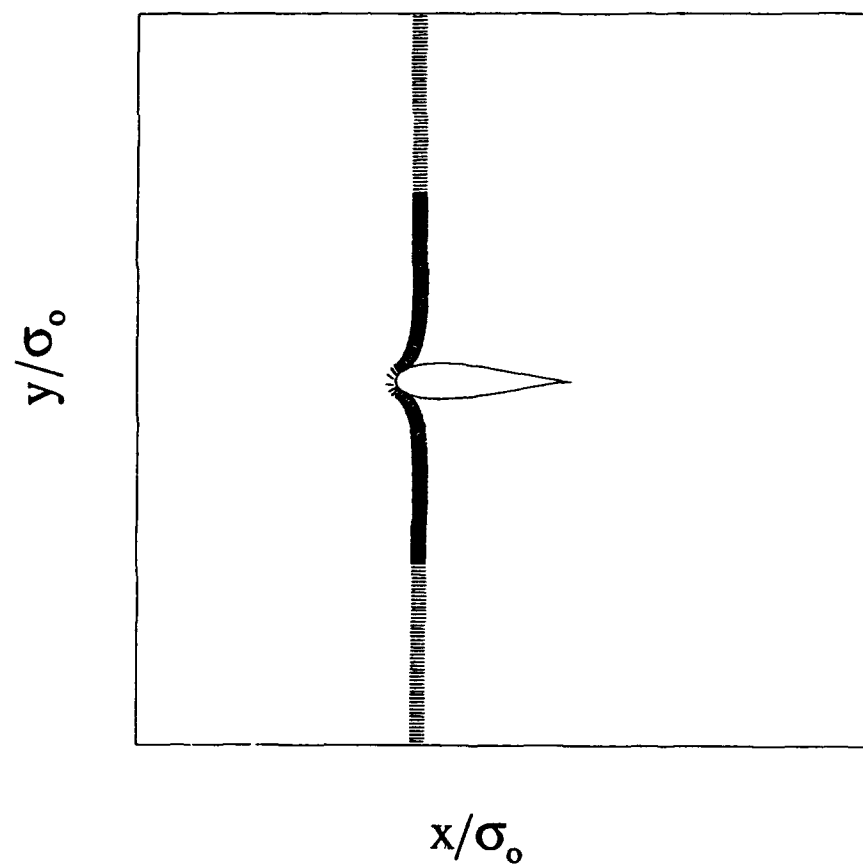


Fig. 5. Side view showing bending (prior to cutting) of a vortex with zero axial flow caused by interaction with a fairly thick blade, with $T/\sigma_0 = 5$ and $2\pi U\sigma_0/\Gamma = 1$, at zero angle of attack.

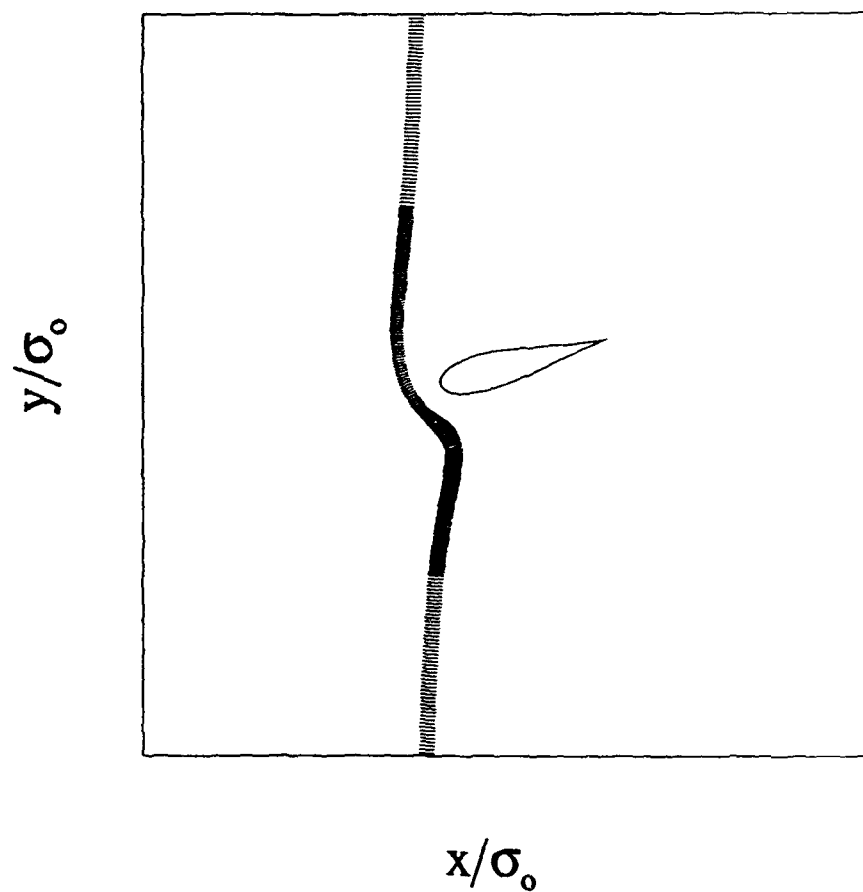


Fig. 6. Side view showing the same case as in Fig. 5, but for a blade with angle of attack $\alpha = -15^\circ$.

kinking of the vortex was not observed for cases with small T/σ_0 , even at fairly large angles of attack.

In order to study in more detail the effect of the ratio $2\pi U\sigma_0/\Gamma$ on the vortex response for large values of T/σ_0 , several computations were performed for the problem of vortex interaction with a circular cylinder of diameter T . It was found that for very small values of $2\pi U\sigma_0/\Gamma$, the vortex will bend towards the cylinder (opposite to the direction of cylinder motion) and impinge on the cylinder surface, as shown in Fig. 7 for the case $T/\sigma_0 = 10$ and $2\pi U\sigma_0/\Gamma = 0.05$. The behavior seems to be due to an instability between the vortex and its image over the cylinder surface, similar in nature to the instability between two parallel vortices with opposite circulation described by Crow (1970).

For large values of $2\pi U\sigma_0/\Gamma$, the vortex is observed to bend away from the cylinder (in the direction of cylinder motion), as shown in Fig. 8 for the case $T/\sigma_0 = 10$ and $2\pi U\sigma_0/\Gamma = 1/2$. In this case, the vortex seems to maintain a minimum distance away from the cylinder leading edge roughly on the order of $T/2$. Impact of the vortex on the cylinder occurs after the cylinder has progressed a much farther distance than was the case for very small values of $2\pi U\sigma_0/\Gamma$, and in this case the vortex impacts on the upper and lower shoulders of the cylinder rather than at the cylinder leading edge. The absence of instability between the vortex and its image for the case of moderate or large values of $2\pi U\sigma_0/\Gamma$ is explained by a theoretical result of Marshall (1992a), in which it is shown that stretching of a vortex pair along its axis (in this case provided by the mean flow about the cylinder) suppresses the Crow instability.

It was also observed that increase in value of $2\pi U\sigma_0/\Gamma$ enhances the decrease in vortex core radius near the leading edge of the cylinder for a given amount of the bending. For instance, a time series of profiles of s along the vortex is shown for two cases in Figs. 9 and 10 for the case $T/\sigma_0 = 10$, for $2\pi U\sigma_0/\Gamma$ values of $1/2$ and 2 , respectively. At the times of the final curves in these two plots, the positions of the vortex axes were nearly identical, and yet the core radius clearly decreases significantly more in the case with larger values of $2\pi U\sigma_0/\Gamma$. The explanation for this behavior is simply that the axial flow within the core, which is driven by variation of core radius, has less time to refill the stretched core when $2\pi U\sigma_0/\Gamma$ is large.

c) Experimental results

An experimental study of the interaction and cutting of an intake vortex with a flat plate blade at various angles of attack and advance speeds has been performed. Experiments were also performed in which circular cylinders of various diameters were towed through the vortex in

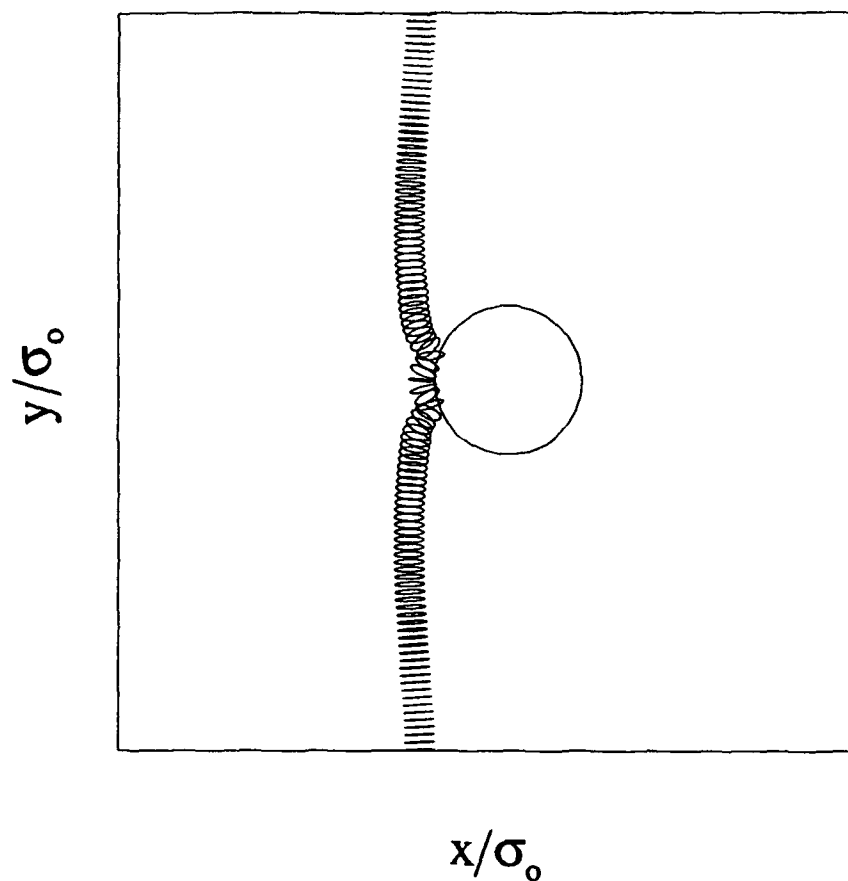


Fig. 7. Side view (looking down the cylinder axis) showing reconnection of the vortex with its image across the cylinder surface for a case with $T/\sigma_0 = 10$, $w_0 = 0$ and slow cylinder forward speed ($2\pi U\sigma_0/\Gamma = 0.05$).

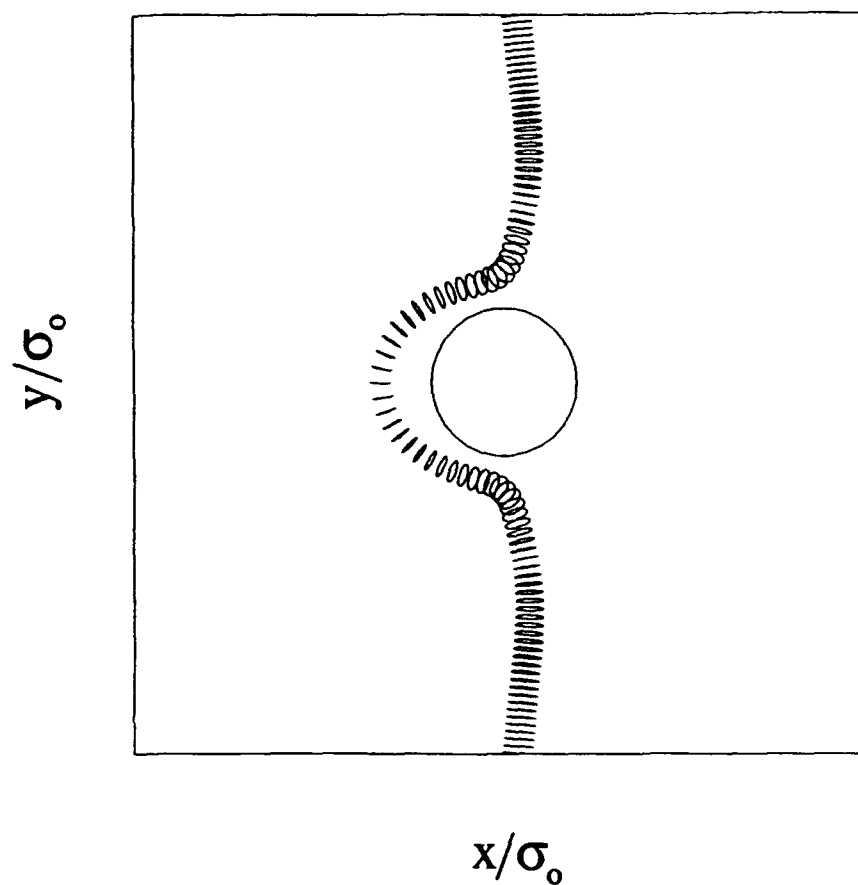


Fig. 8. Side view showing the bending of a vortex with no axial flow caused by interaction with a circular cylinder for a case with $T/\sigma_0 = 10$ and a larger cylinder forward speed ($2\pi U\sigma_0/\Gamma = 1/2$).

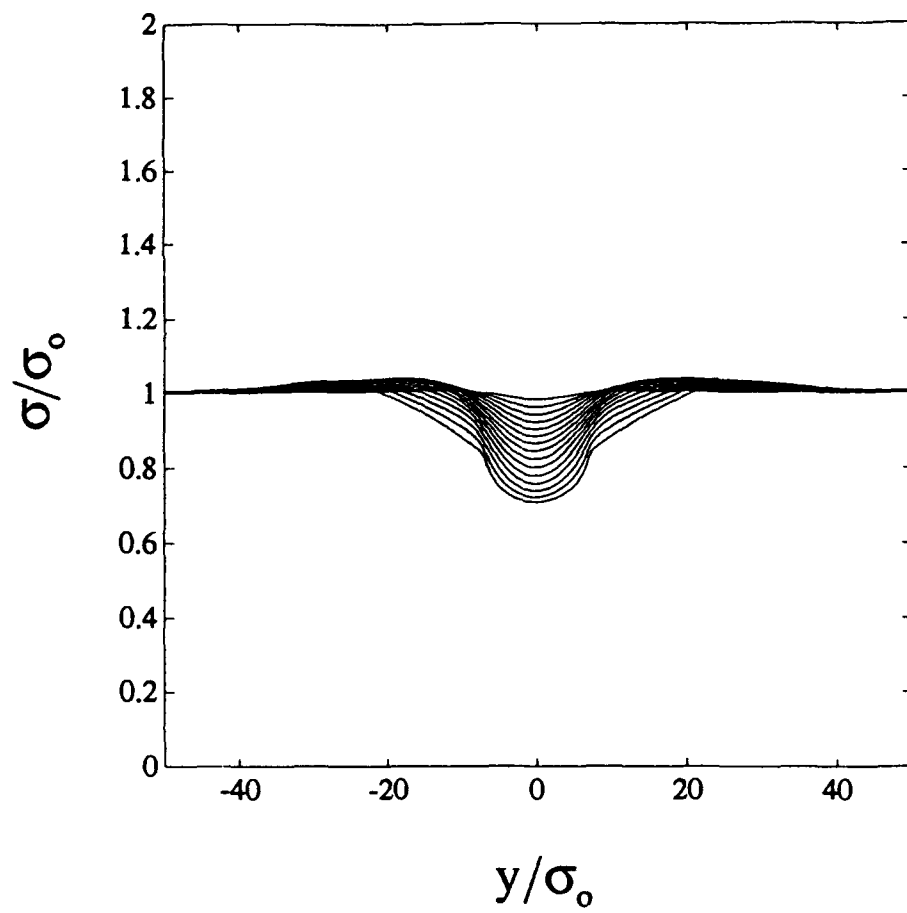


Fig. 9. Variation of vortex core radius with distance along the vortex axis at a series of times for the same run as shown in Fig. 8.

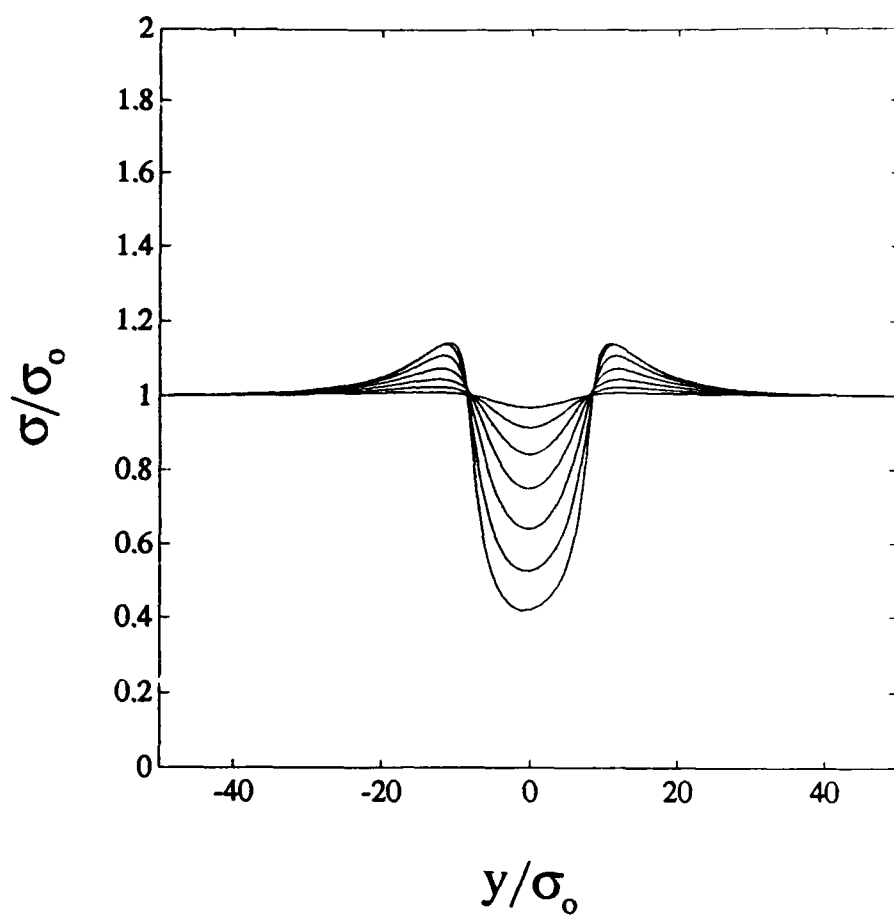


Fig. 10. Variation of vortex core radius with distance along the vortex axis at a series of times for a case with $T/\sigma_0 = 10$ and a large cylinder forward speed ($2\pi U\sigma_0/\Gamma=2$). Comparison of Fig. 9 and 10 shows the effect of cylinder forward speed on decrease in vortex core radius.

place of the blade. The experimental apparatus is shown in Fig. 11, and details can be found in Marshall and Krishnamoorthy (1993). All flow measurements were made from video photographs of passive dye globules at various locations within the flow, as well as of dye (of a different color) marking the vortex core. The blade was mounted on a carriage and driven by a variable speed motor.

The main objectives of the experiments were both to check the accuracy of the theoretical and computational predictions and to examine the nature and structure of vortex shocks. It was observed in all experiments with cutting of the vortex by a blade that an abrupt disturbance of the vortex core forms on the compression side of the vortex and propagates rapidly away from the blade (upstream), while no noticeable disturbance of this type is observed on the expansion side of the vortex. Very close to the blade the dye within the vortex core (on both sides of the blade) seems to disappear, and the length of the region in which the dye was absent increases with time. This depletion of dye (in the vortex core) near the blade is attributed to suction of boundary layer fluid into the vortex core (although to confirm this further experiments need to be performed in which the blade boundary layer fluid is visualized as well).

The abrupt vortex disturbance on the compression side of the vortex seems to adopt one of two structural forms, as shown in Figs. 12a and 12b. The disturbance in Fig. 12a appears similar to a spiral-type traveling vortex breakdown and that in Fig. 12b appears similar to a bubble-type traveling vortex breakdown followed by a forking of the vortex into a double-helix shape. (Comparison can be made, for instance, with flow visualization results of Sarpkaya (1971) or Faler and Leibovich (1977) for vortex breakdowns in diverging tubes.)

The propagation speed of the vortex disturbance can be readily measured and is plotted in terms of dimensionless quantities in Fig. 13. The solid curve in this figure is the theoretical prediction for vortex shocks obtained from Eqs. (10) and (11), and the data are given for laminar vortices with zero angle of attack ('o'), laminar vortices with non-zero angle of attack ('*') and vortices with highly turbulent cores ('+'). It is noted that the data represent a variation of shock speed by a factor of over seven, whereas the dimensionless data vary from their theoretical values by no more than thirty percent. The experimental uncertainty in Fig. 13 is fairly high, about ± 0.1 on the vertical axis and ± 0.05 on the horizontal axis, mainly due to uncertainty in determination of the ambient core radius. Also, the theoretical curve does not account for suction of blade boundary layer fluid into the vortex core, which is believed to be considerable.

In light of these considerations, the rough agreement between the theoretical prediction for vortex shock speed and the measured speed of the vortex disturbances, together with the

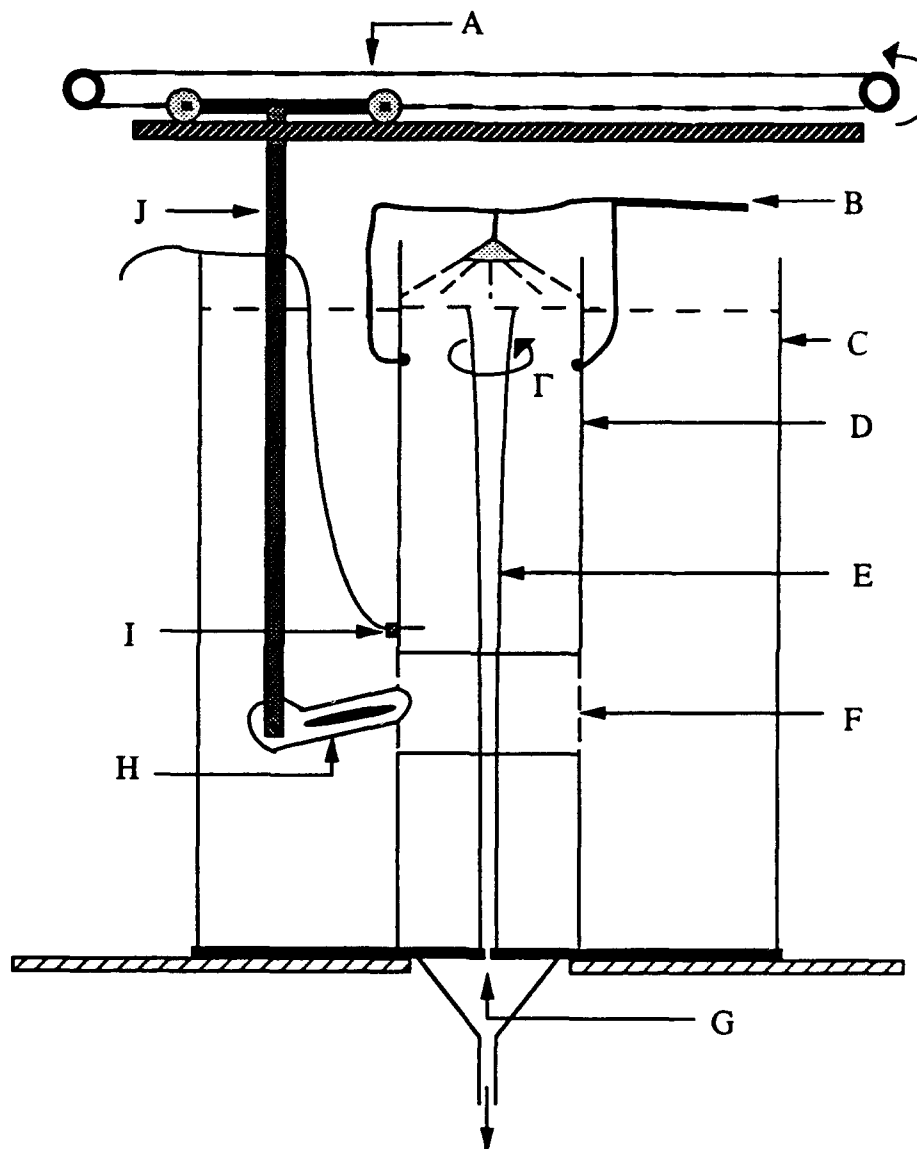


Fig. 11. Schematic of the experimental configuration: A, tow carriage driven by variable speed motor; B, water inlet into azimuthally oriented jets with optional shower head inlet; C, outer rectangular tank; D, inner cylindrical tank; E, vortex core; F, gap left to allow passage of blade (or circular cylinder) with flexible plastic strips; G, orifice at tank bottom; H, thin blade (or circular cylinder) mounted at adjustable angle of attack; I, hypodermic needle to inject dye globules for circulation measurement; J, support arms for carriage.



(a)



(b)

Fig. 12. Pictures showing the structure of vortex shocks of two different forms, both generated by cutting the vortex by a thin blade with zero angle of attack. A spiral shock is shown in (a) for the case $2\pi w_0 \sigma_0 / \Gamma = -0.26$ and $2\pi U \sigma_0 / \Gamma = 0.19$. A shock with bubble-type breakdown, which spirals in a double-helix form downstream, is shown in (b) for the case $2\pi w_0 \sigma_0 / \Gamma = -0.16$ and $2\pi U \sigma_0 / \Gamma = 0.036$. The dimensionless shock speed $2\pi \sigma_0 W / \Gamma$ is found to be 0.40 in (a) and 0.61 in (b).

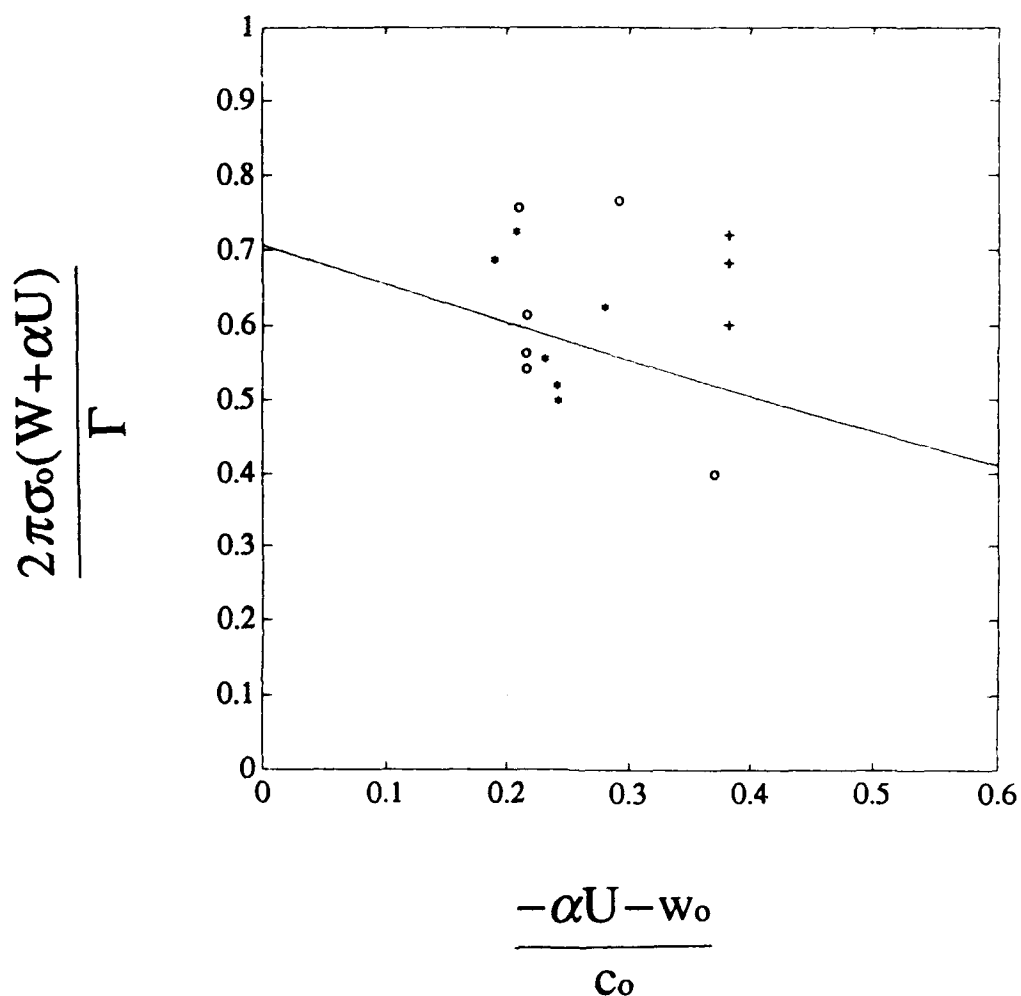


Fig. 13. Comparison of experimental data for shock speed, plotted in terms of the dimensionless parameter $2\pi\sigma_0(W+\alpha U)/\Gamma$, with the analytical solution (solid curve) assuming no suction of blade boundary layer fluid into the vortex. The data points for a blade with angle of attack $\alpha=0$ are marked by a circle 'o', those for a blade with finite α are marked by a star '*', and those taken using the shower head to inlet part of the flow (for which case the vortex has high turbulence intensity) are marked by a plus sign '+'.

observation that such disturbances only occur on the compression side of the vortex, strongly implies that the observed vortex disturbance is a manifestation of a vortex shock. Further, the observed similarity in form of the vortex disturbances due to cutting and vortex breakdowns reported in various circumstances in the literature suggests that perhaps vortex breakdowns in general are simply manifestations of vortex shocks. This proposal has been suggested previously in the literature (Lundgren and Ashurst, 1989, Marshall, 1991), and is supported also by the observation that vortex shocks seem to be predicted theoretically in a range of situations in which vortex breakdowns are observed in experiments, including cases in which a vortex is exposed to an external adverse pressure gradient as would occur for a vortex confined in the center of a diverging tube (Marshall, 1993a).

Experiments with vortices interacting with circular cylinders were also performed and compared to computational results performed with the same values of the dimensional parameters governing the system. The experimental and computational results agreed closely up until the point (at low values of $2\pi U\sigma_0/\Gamma$) at which the computations predict the vortex to impact on the cylinder surface due to instability with its image vortex. At this point the experiments also indicate that the vortex bends back toward the cylinder surface, but then instead of impacting with the surface at two distinct points (as in the computations) the experiments show a cascade of vortex wave energy to progressively smaller scales. Thus, at first one wave on the vortex will form, which evolves into two spiraling waves, which evolves into four waves, and so on. This formation of waves of increasing smaller length occurs quite rapidly, so that by the time the vortex impacts on the surface there may be ten or more spiraling waves on the vortex axis which all impact with the cylinder at nearly the same time. (The exact number of waves of course varies with T/σ_0 and $2\pi U\sigma_0/\Gamma$.) After the vortex impacts the cylinder surface, it seems to rapidly disrupt and the dye quickly disperses.

d) Conclusions

The long-wave theory of vortex filaments with variable core radius has been found to give reliable results for numerical computations, both in comparison to experiments and to results of more exact numerical computations (Marshall and Grant, 1993), in a variety of situations in which variation of the vortex core radius along the vortex axis is important. For the problem of vortex cutting by blades, an analytical solution of this theory for straight vortices seems to correctly predict many of the important flow features (such as vortex shock formation and propagation speed) for values of the ratio T/σ_0 of $O(1)$ or smaller. For large values of T/σ_0 , significant bending of the vortex occurs prior to cutting, but even for this case computational

solutions using this long-wave vortex filament theory compare well with experiments with the exception of some details involving vortex impact on the blade surface.

For large values of T/σ_0 , it thus seems that acoustic theories of blade-vortex interaction noise at normal incidence with a blade at zero angle of attack which assume the vortex to remain circular and stretch about the blade leading edge (such as that of Howe, 1989) should be fairly accurate, up until the point of vortex impact on the blade surface, although a correction should be made in such theories to account for decrease in vortex core diameter as it is stretched by the blade, which can be substantial for large values of $2\pi U\sigma_0/\Gamma$. For cases with large T/σ_0 values and blades at a moderate (non-zero) angle of attack, a kinking of the vortex is observed which is expected to significantly affect blade sound generation. A more detailed experimental study of this kinking phenomenon needs to be made.

For cases with T/σ_0 values of $O(1)$ or smaller, which is typical of helicopter applications, there are several points which require further investigation. The most urgent need is to examine the nature of the cutting process itself, which was assumed to occur instantaneously in the present theoretical work. In particular, the question of whether a large impulsive force is exerted on the blade during cutting of the vortex or whether the force varies monotonically from its value before cutting to that after cutting (such that the sound generation can be estimated from the present theory) should be resolved. Also, there would be some value in investigating further the proposed relationship between vortex shocks and vortex breakdown, including the question of whether the determination of structural form of the breakdown can be associated with instabilities predicted by the simple vortex filament theory, such as vortex "buckling" (Marshall, 1992b) which might develop due to compression of the vortex axis within the shock. Finally, the suction of blade boundary layer fluid into the vortex after cutting has occurred is a relatively untouched problem (for moving blades) which merits further study.

LIST OF PUBLICATIONS AND TECHNICAL REPORTS

The following publications have been written and submitted as a result of this project.

1. Marshall, J.S., and Grant, J.R., *Evolution and breakup of vortex rings in straining and shearing flows*, submitted to J. Fluid Mech.
2. Marshall, J.S., *Vortex cutting by a blade. Part I. General theory and a simple solution*, AIAA J. (in press).
3. Marshall, J.S., and Yalamanchili, R., *Vortex cutting by a blade. Part II. Computations*, submitted to AIAA J.
4. Marshall, J.S., and Krishnamoorthy, S., *Vortex cutting by a blade. Part III. Experiments*, submitted to AIAA J.
5. Marshall, J.S., *Vortex cutting by a blade*, talk to be presented at the 46th Annual Meeting of the Division of Fluid Dynamics of the American Physical Society, Albuquerque, NM, November 1993 (abstract).

LIST OF PARTICIPATING SCIENTIFIC PERSONNEL

1. J.S. Marshall (Principal Investigator).
2. S. Krishnamoorthy, M.S. degree expected in December 1993 from the Ocean Engineering Department at Florida Atlantic University. Thesis title: *An experimental study of vortex response during cutting by a blade or cylinder.*
3. R. Yalamanchili, M.S. degree expected in December 1993 from the Ocean Engineering Department at Florida Atlantic University. Thesis title: *Computations of normal vortex interaction with blades and circular cylinders.*

REPORT OF INVENTIONS

No inventions were made in the course of this project.

BIBLIOGRAPHY

1. Ahmadi, A.R., *An experimental investigation of blade-vortex interaction at normal incidence*, AIAA J. Aircraft, Vol. 23, 1986, pp. 47-55.
2. Amiet, R.K., *Airfoil gust response and the sound produced by airfoil-vortex interaction*, J. Sound Vibration, Vol. 107, 1986, pp. 487-506.
3. Cary, C.M., *An experimental investigation of the chopping of helicopter main rotor tip vortices by the tail rotor. Part II. High speed photographic study*, NASA CR-177457, 1987.
4. Crow, S.C., *Stability theory for a pair of trailing vortices*, AIAA J. Vol. 8, 1970, pp. 2172-2179.
5. Faler, J.H., and Leibovich, S., *Disrupted states of vortex flow and vortex breakdown*, Phys. Fluids, Vol. 20, 1977, pp. 1385-1400.
6. Howe, M.S., *Contributions to the theory of sound production by vortex-airfoil interaction, with application to vortices with finite axial velocity defect*, Proc. R. Soc. Lond. A, Vol. 420, 1988, pp. 157-182.
7. Howe, M.S., *On unsteady surface forces, and sound produced by the normal chopping of a rectilinear vortex*, J. Fluid Mech., Vol. 206, 1989, pp. 131-153.
8. Leverton, J.W., Pollard, J.S., and Wills, C.R., *Main rotor wake/tail rotor interaction*, Vertica, Vol. 1, No. 3, 1977, pp. 213-221.
9. Lewis, R.I., Vortex Element Methods for Fluid Dynamic Analysis of Engineering Systems, Camb. Univ. Press, Cambridge, U.K., 1991.
10. Lundgren, T.S., and Ashurst, W.T., *Area-varying waves on curved vortex tubes with application to vortex breakdown*, J. Fluid Mech., Vol. 200, 1989, pp. 283-307.
11. Marshall, J.S., *A general theory of curved vortices with circular cross-section and variable core area*, J. Fluid Mech., Vol. 229, 1991, pp. 311-338.

12. Marshall, J.S., *The effect of axial stretching on the three-dimensional stability of a vortex pair*, J. Fluid Mech., Vol. 241, 1992a, pp. 403-419.
13. Marshall, J.S., *Buckling of a columnar vortex*, Phys. Fluids A, Vol. 4, 1992b, pp. 2620-2627.
14. Marshall, J.S., *The effect of axial pressure and gradient on axisymmetrical and helical vortex waves*, Phys. Fluids A, Vol. 5, 1993a, pp. 588-599.
15. Marshall, J.S., *Vortex cutting by a blade. Part I. General theory and a simple solution*, AIAA J., 1993b, in press.
16. Marshall, J.S., and Grant, J.R., *Evolution and breakup of vortex rings in straining and shearing flows*, submitted to J. Fluid Mech.
17. Marshall, J.S., and Krishnamoorthy, S., *Vortex cutting by a blade. Part III. Experiments*, submitted to AIAA J.
18. Marshall, J.S., and Yalamanchili, R., *Vortex cutting by a blade. Part II. Computations*, submitted to AIAA J.
19. Moore, D.W., *Finite amplitude waves on aircraft trailing vortices*, Aeronaut. Quart., Vol. 23, 1972, pp. 307-314.
20. Moore, D.W. and Saffman, P.G., *The motion of a vortex filament with axial flow*, Phil. Trans. R. Soc. Lond. A, Vol. 272, 1972, pp. 403-429.
21. Sarpkaya, T., *On stationary and traveling vortex breakdown*, J. Fluid Mech., Vol. 45, 1971, pp. 545-559.
22. Weigand, A., *Response of a vortex ring to a transient, spatial cut*, Ph.D. dissertation, Univ. of California, San Diego, 1993.